

22nd Conference on Flavor Physics and CP Violation (FPCP 2024)
May 30, 2024 @ Chulalongkorn University

Theoretical progress in CP violation in D -meson system

Cheng-Wei Chiang
National Taiwan University
National Center for Theoretical Sciences



The Acclaimed Dark Horse

Bigi and Sanda, *CP Violation*, Chapter 14

- CP violation in charm decays is considered as the **dark horse**.

“... charm’s SM phenomenology provides us with **a dual opportunity**, namely to

- (1) probe our *quantitative* understanding of **QCD’s non-perturbative dynamics** thus calibrating our theoretical tools for describing B decays;
- (2) perform almost ‘zero-background’ searches for **New Physics**, mainly in the area of **CP violation**.”

The Acclaimed Dark Horse

Bigi and Sanda, *CP Violation*, Chapter 14

- CP violation in charm decays is considered as the **dark horse**.

“... charm’s SM phenomenology provides us with **a dual opportunity**, namely to

- (1) probe our *quantitative* understanding of **QCD’s non-perturbative dynamics** thus calibrating our theoretical tools for describing B decays;
- (2) perform almost ‘zero-background’ searches for **New Physics**, mainly in the area of **CP violation**.”

- Have we fully understood these two aspects?

The Acclaimed Dark Horse

Bigi and Sanda, *CP Violation*, Chapter 14

- CP violation in charm decays is considered as the **dark horse**.

“... charm’s SM phenomenology provides us with **a dual opportunity**, namely to

- (1) probe our *quantitative* understanding of **QCD’s non-perturbative dynamics** thus calibrating our theoretical tools for describing B decays;
- (2) perform almost ‘zero-background’ searches for **New Physics**, mainly in the area of **CP violation**.”

- Have we fully understood these two aspects?



Importance of Hadronic D Meson Decays

- D mesons decay dominantly ($\sim 84\%$) into **hadronic** final states, 3/4 of which are two-body modes.

⇒ importance of hadronic decay modes in understanding the D meson

Mode	BR
PP	$\sim 10\%$
VP	$\sim 28\%$
VV	$\sim 10\%$
SP	$\sim 4.2\%$
AP	$\sim 10\%$
TP	$\sim 0.3\%$
2-body	$\sim 63\%$
hadronic	$\sim 84\%$
semileptonic	$\sim 16\%$

— most dominant ones

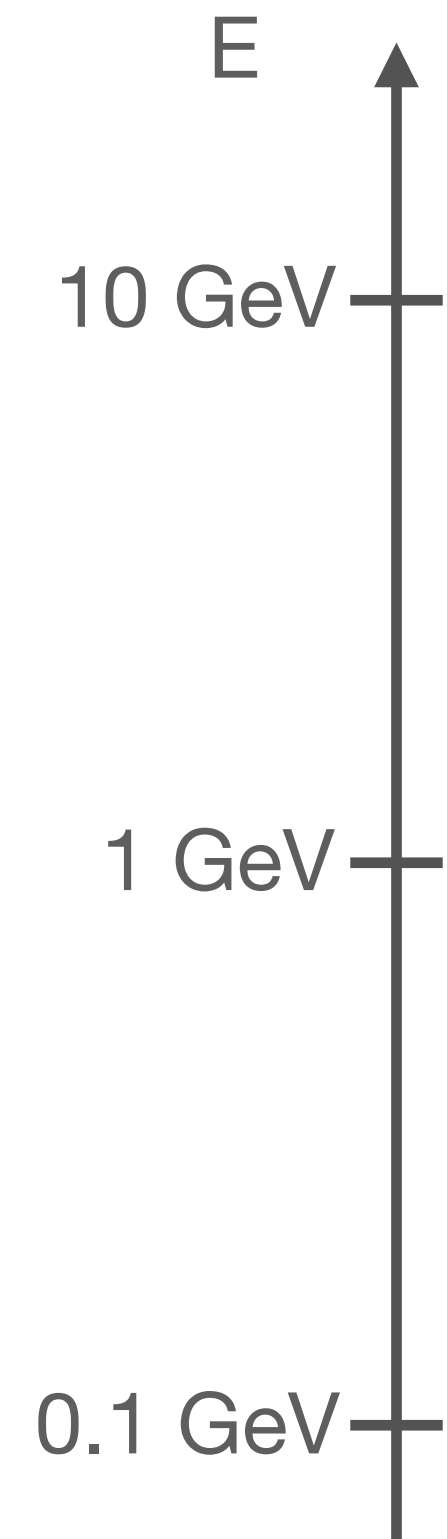
P: pseudoscalar meson

V: vector meson

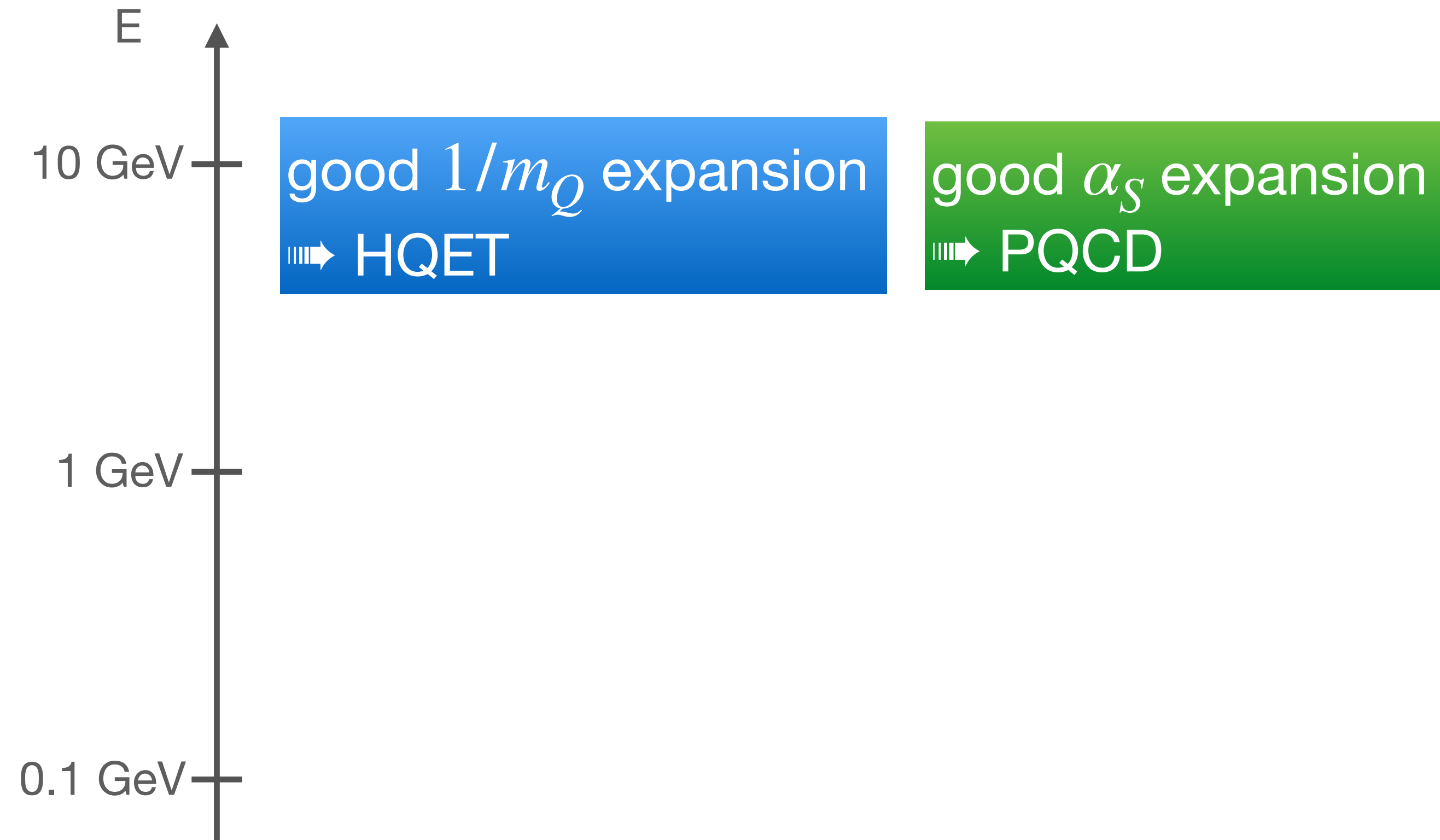
A: axial vector meson

T: tensor meson

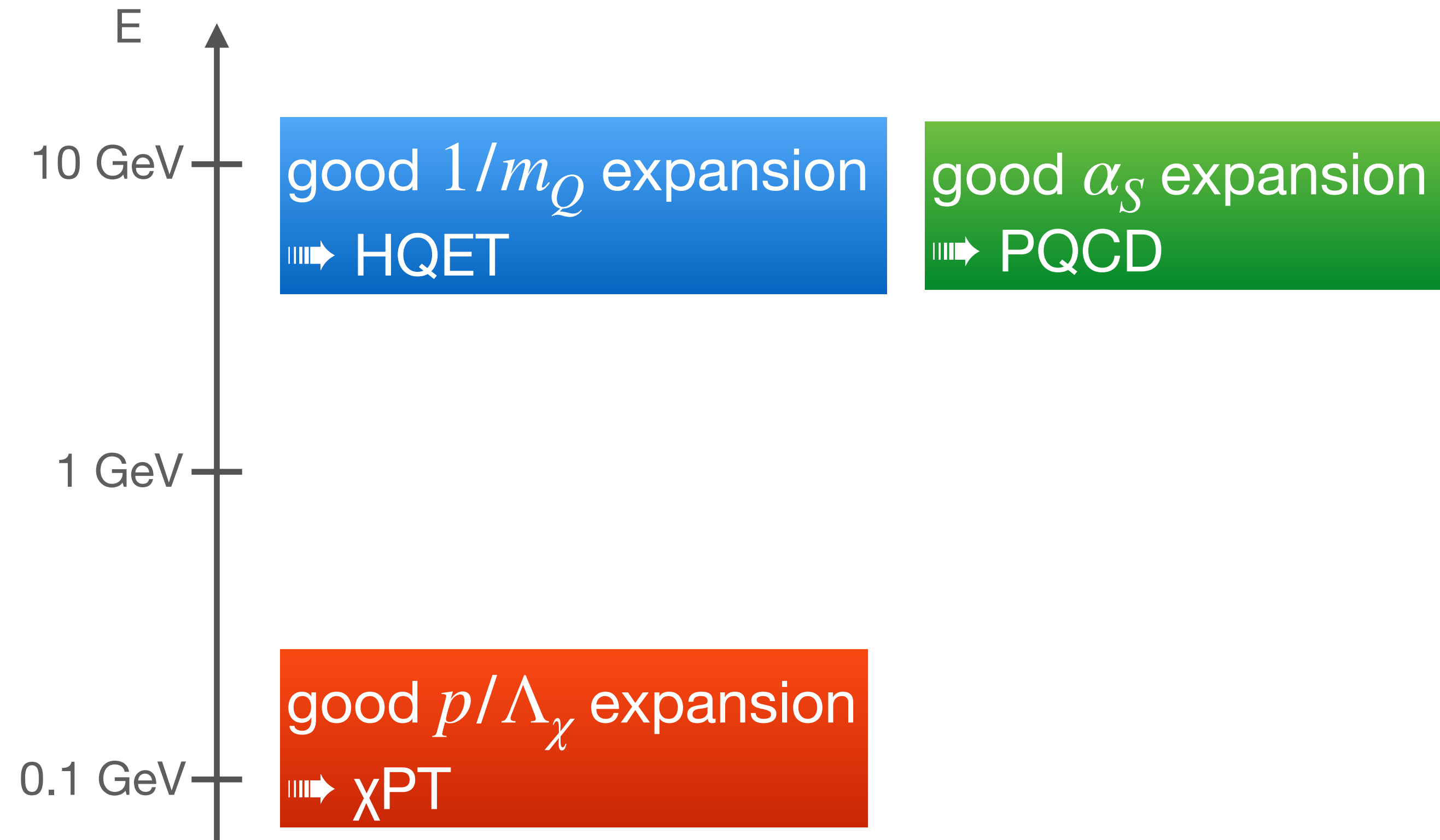
Peculiarities of Charm System



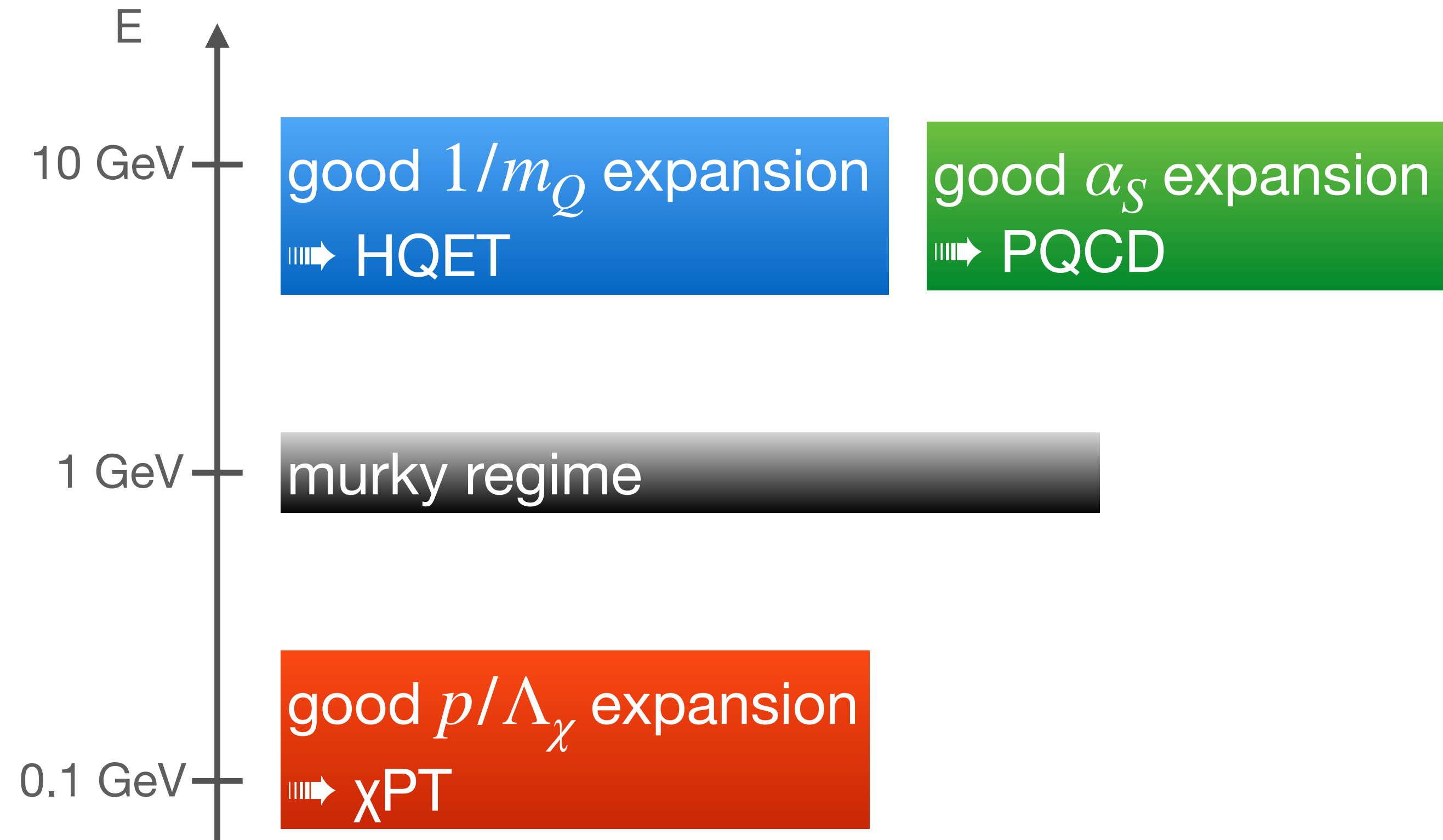
Peculiarities of Charm System



Peculiarities of Charm System

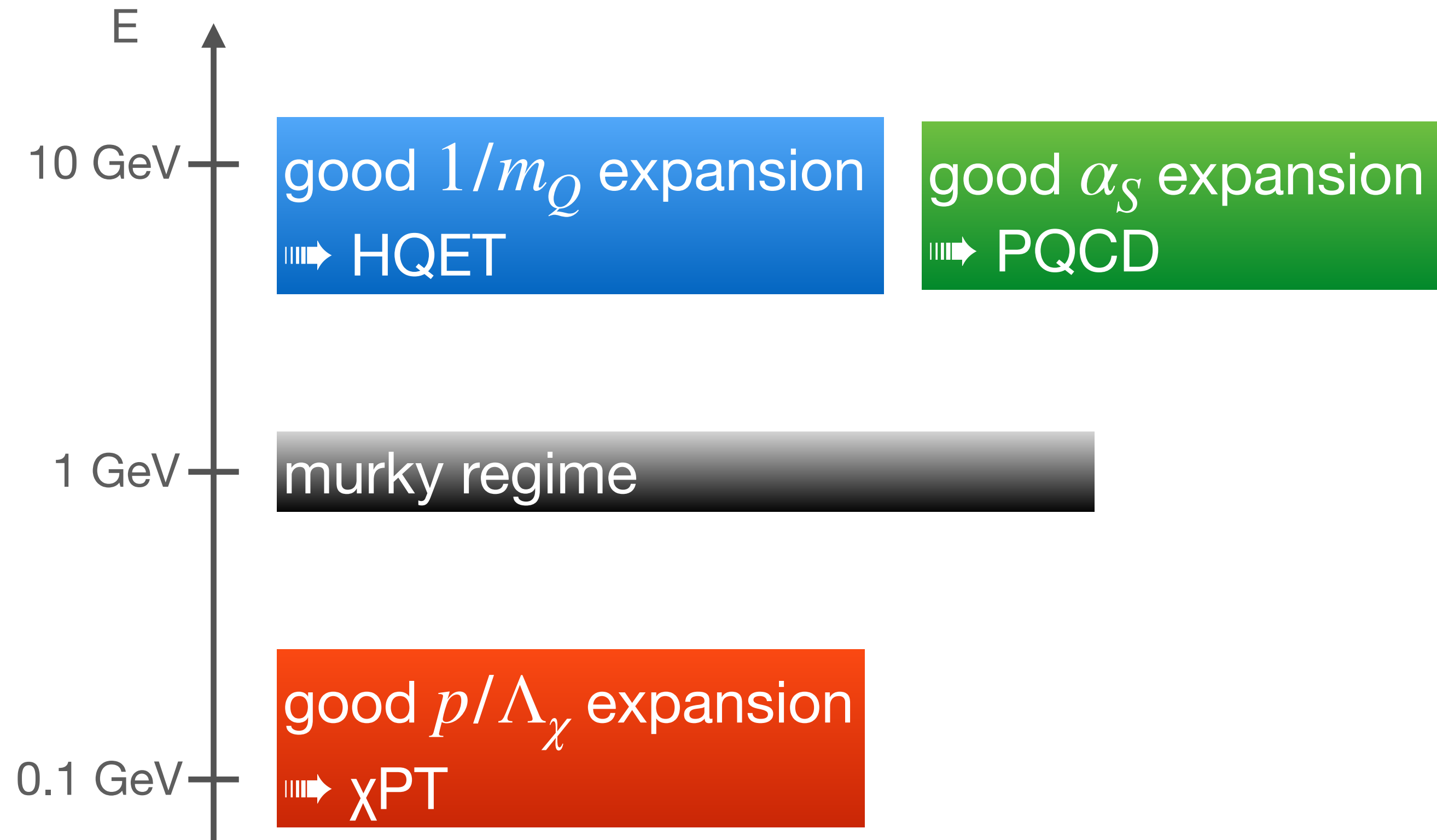


Peculiarities of Charm System



- $\Lambda_{\text{QCD}}/m_c \sim 0.3$
 - ▮ bad heavy quark expansion
 - ▮ higher power corrections
- $\alpha_S(m_c) \sim 0.3$
 - ▮ bad PQCD expansion
 - ▮ higher-order perturbations and/or nonperturbative effects
- Many nearby resonances
 - ▮ final-state rescattering effects

Peculiarities of Charm System



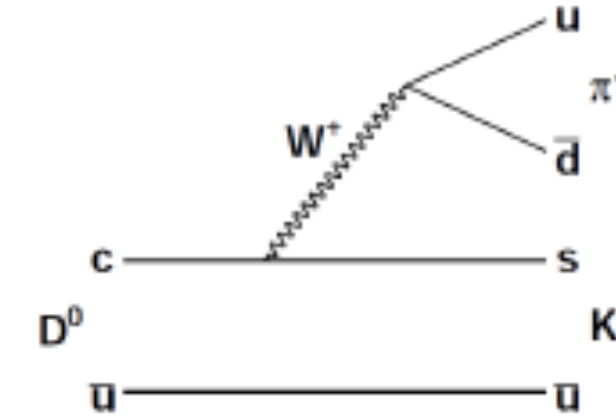
- $\Lambda_{\text{QCD}}/m_c \sim 0.3$
 - ▮▮▮▮ bad heavy quark expansion
 - ▮▮▮▮ higher power corrections
- $\alpha_S(m_c) \sim 0.3$
 - ▮▮▮▮ bad PQCD expansion
 - ▮▮▮▮ higher-order perturbations and/or nonperturbative effects
- Many nearby resonances
 - ▮▮▮▮ final-state rescattering effects

- There is **no satisfactory effective theory** that allows us to study the charm system reliably, particularly for the **hadronic decays**.
- Common approaches: **symmetry-based** and **perturbation-based**, assisted with lattice inputs and sometimes **phenomenological** models.

Cabibbo Hierarchy in Hadronic D Decays

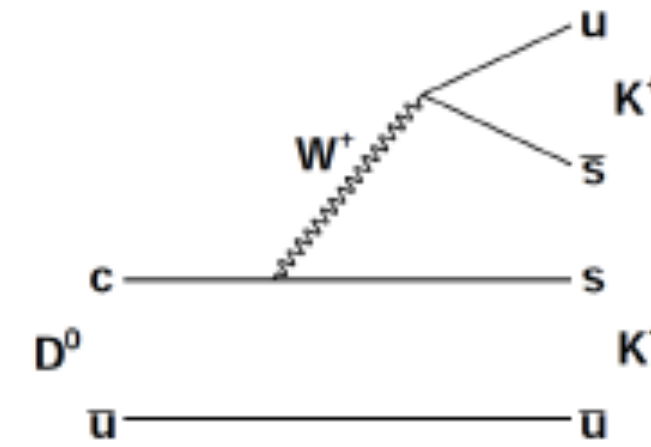
- Cabibbo-favored (CF):

$$\text{involving } V_{cs}^* V_{ud} \sim 1 - \lambda^2 \sim 0.95$$



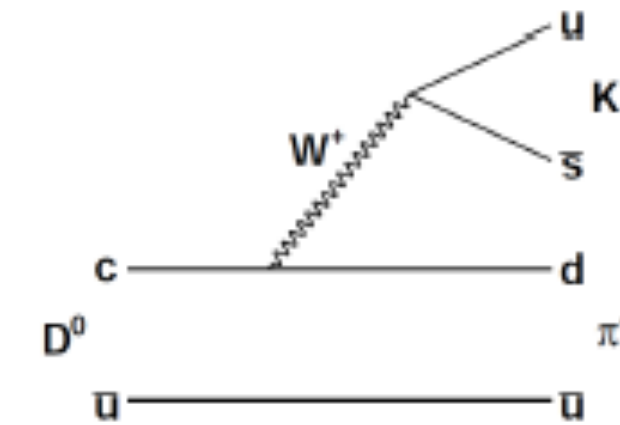
- Singly Cabibbo-suppressed (SCS):

$$\text{involving } V_{cd}^* V_{ud} \text{ or } V_{cs}^* V_{us} \sim \lambda \sim 0.22$$



- Doubly Cabibbo-suppressed (DCS):

$$\text{involving } V_{cd}^* V_{us} \sim \lambda^2 \sim 0.05$$



- **SCS decays** can involve diagrams with different CKM phases and have **CPA's**:

$$\text{Amp} = V_{cd}^* V_{ud} (\text{trees} + \text{penguins}) + V_{cs}^* V_{us} (\text{trees} + \text{penguins})$$

|
|

tiny relative weak phase between the two combinations

(after using unitarity identity)

GIM Mechanism

- In the SM, the CKM matrix takes the hierarchical form: Cabibbo 1963; Kobayashi, Maskawa 1973
Wolfenstein 1983

$$V_{\text{CKM}} = \begin{pmatrix} V_{ud} & V_{us} & V_{ub} \\ V_{cd} & V_{cs} & V_{cb} \\ V_{td} & V_{ts} & V_{tb} \end{pmatrix} \simeq \begin{pmatrix} 1 - \frac{\lambda^2}{2} & \lambda & A\lambda^3(\rho - i\eta) \\ -\lambda & 1 - \frac{\lambda^2}{2} & A\lambda^2 \\ A\lambda^3[(1 - \bar{\rho}) - i\bar{\eta}] & -A\lambda^2 & 1 \end{pmatrix}$$

where the unitarity condition for the upper two rows (relevant for charm physics)

$$\lambda_d + \lambda_s + \lambda_b = 0 \quad (\text{where } \lambda_q \equiv V_{cq}^* V_{uq})$$

renders an **extremely squashed unitarity triangle** (roughly $1 : 1 : 10^{-3}$ sides).

- The loop function for the $c \rightarrow u$ penguin amplitude $\sim \frac{1}{(4\pi)^2} \frac{m_q^2}{m_W^2}$, which is of order $(10^{-10}, 10^{-8}, 10^{-5})$ for the $d, s,$ and b quark, respectively, resulting in a **very effective Glashow-Iliopoulos-Maiani (GIM) cancellation**.

CP Violation in SCS Decays

- Typically, direct CPA's in SCS decays are given by

$$a_{\text{CP}}^{\text{dir}} = \frac{2\text{Im}(V_{cd}^* V_{ud} V_{cs} V_{us}^*)}{|V_{cd}^* V_{ud}|^2} \left| \frac{A_2}{A_1} \right| \sin \delta = 2 \left| \frac{V_{cb}^* V_{ub}}{V_{cd}^* V_{ud}} \right| \sin \gamma \left| \frac{A_2}{A_1} \right| \sin \delta \sim 10^{-3} \left| \frac{A_2}{A_1} \right| \sin \delta$$

relative strong phase
|
weak phase of V_{ub}^*
|

where A_1 and A_2 generically denote amplitudes (including tree and penguin types in general) associated with different CKM factors.

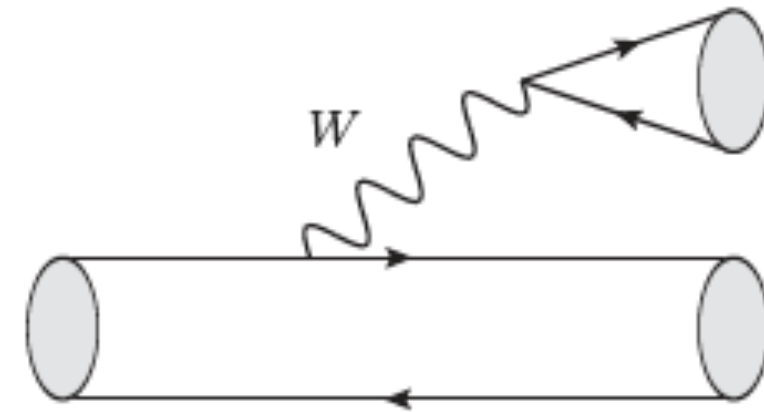
- With $|A_2/A_1| \lesssim 1$, the CPA is at most $\mathcal{O}(10^{-3})$.
 - ▣▣▣▣ new physics, if measured to be more sizable
 - ▣▣▣▣ current data at the borderline...
- The estimates of $|A_2/A_1|$ differ between perturbative and symmetry approaches.

Symmetry-based Approach – Topological Diagrams

- Diagrams for 2-body hadronic D meson decays can be classified more intuitively according to **flavor topology** into the tree- and loop-types, universal in **flavor SU(3) limit**:

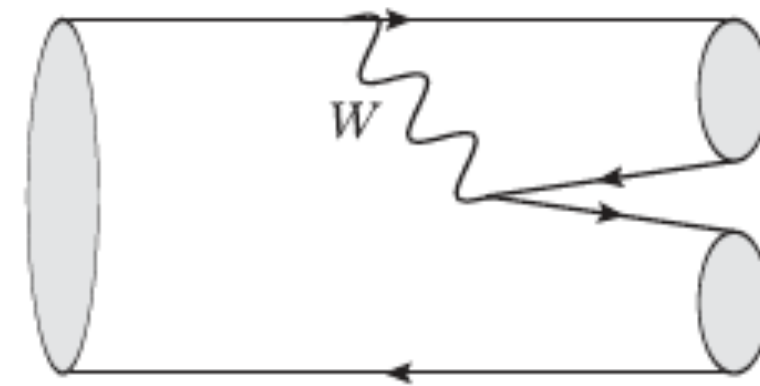
Zeppenfeld 1981
 Chau and Cheng 1986, 1987, 1991
 Savage and Wise 1989
 Grinstein and Lebed 1996
 Gronau et. al. 1994, 1995, 1995

Tree-type



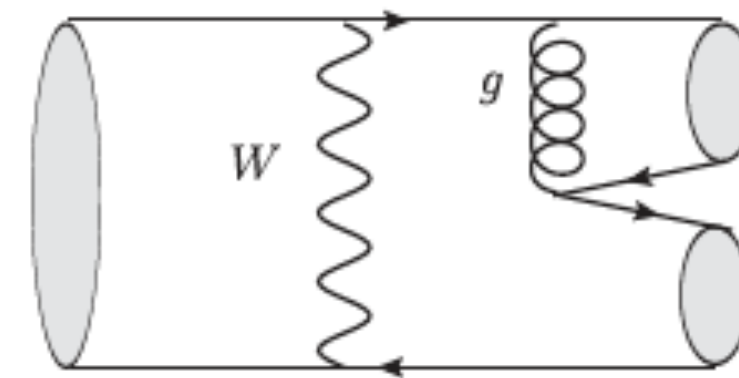
(a) T

color-allowed tree



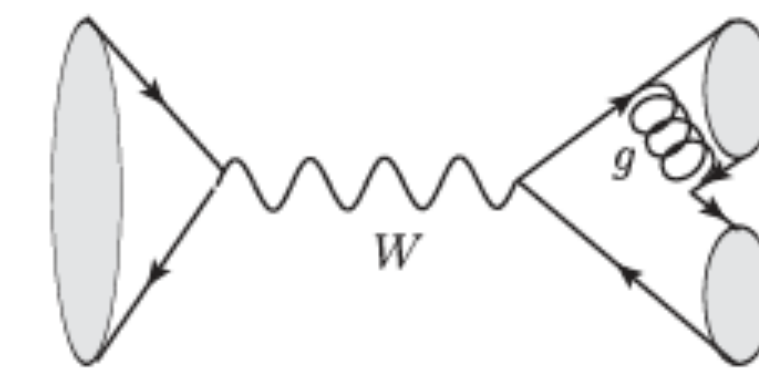
(b) C

color-suppressed tree



(e) E

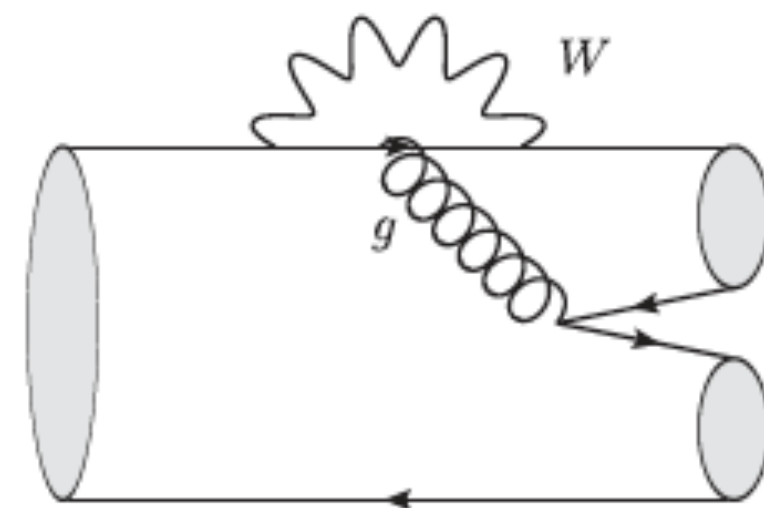
exchange



(f) A

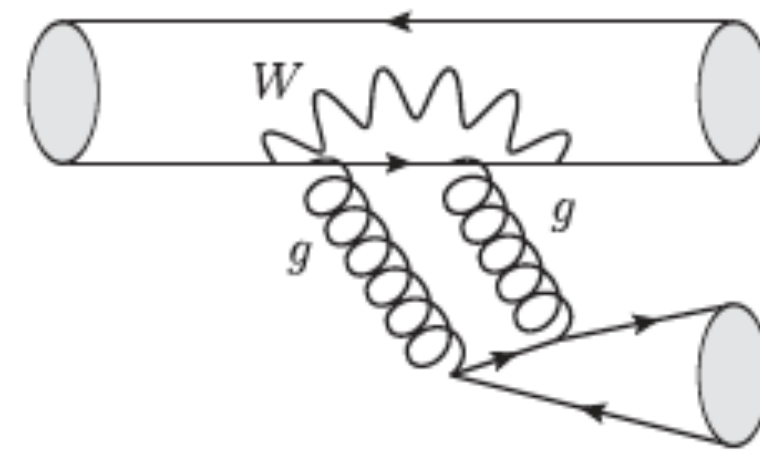
annihilation

Loop-type



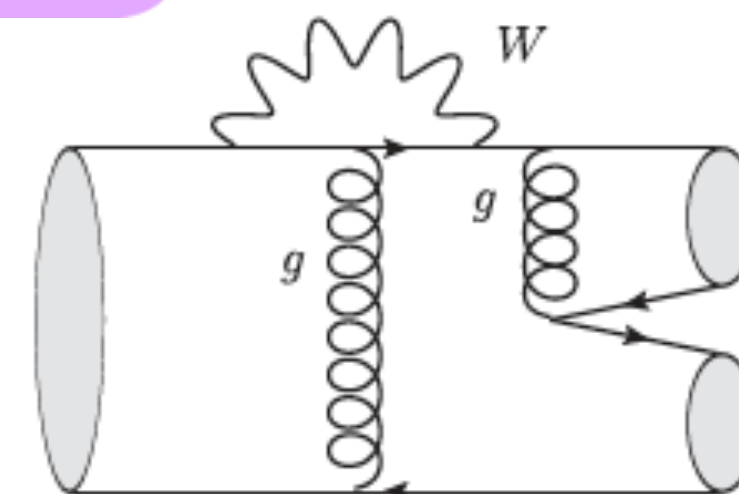
(c) P, P_{EW}^C

QCD penguin
 color-suppressed EW penguin



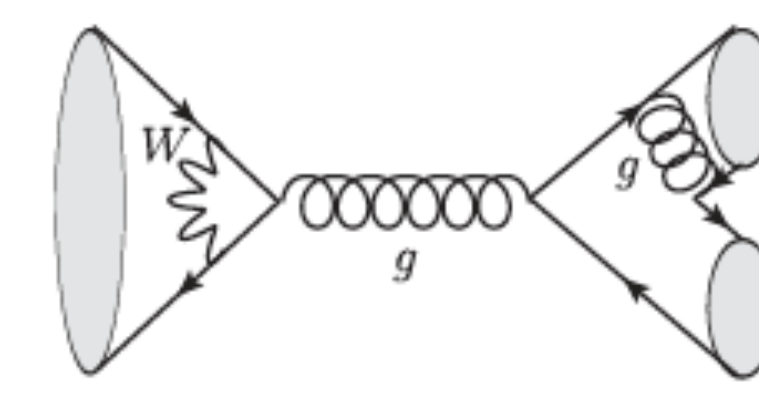
(d) S, P_{EW}

singlet penguin
 EW penguin



(g) PE, PE_{EW}

penguin exchange
 EW penguin exchange



(h) PA, PA_{EW}

penguin annihilation
 EW penguin annihilation

From Partial Width to Decay Amplitude

- Partial decay widths of $D \rightarrow PP$ and VP decays are related to their decay amplitudes as follows:

$$\Gamma(D \rightarrow PP) = \frac{p_c}{8\pi m_D^2} |\mathcal{M}|^2$$

magnitude of 3-momentum
 of final-state particle
 |

$$\Gamma(D \rightarrow VP) = \frac{p_c^3}{8\pi m_V^2} |\mathcal{M}|^2$$

P-wave state
 |
 due to polarization sum

- Flavor SU(3) breaking due to **phase space difference** is thus removed.
- In the symmetry limit, flavor SU(3) is assumed **at the amplitude level** (**decay strength** and **strong phase**), where the decay amplitude \mathcal{M} is a linear combination of the topological amplitudes multiplied by the corresponding CKM factors.

Symmetry-based Approach

- As far as BR's are concerned, penguin diagrams are **negligible** because of the **GIM mechanism** ($V_{cd}^* V_{ud} = -V_{cs}^* V_{us}$ and $V_{cb}^* V_{ub} \sim A^2 \lambda^5$).
 - ▮ **tree-type** diagrams are dominant in determining the BR's
- Perform a χ^2 fit to the BR's of all **CF** modes, extracting **magnitudes** and **strong phases** (up to discrete ambiguities) of all the topological amplitudes.
- Make **flavor SU(3) symmetry-breaking corrections** (mostly in the magnitude) as demanded by data.
- Include penguin amplitudes, particularly certain diagrams that could be enhanced by **final-state rescattering**, to induce large direct CPA's.
- Using the extracted information, make predictions of BR's and CPA's for SCS and DCS modes.
 - ▮ **testable by current/future data**

Tree-level Amplitudes and Long-distance Effects

- A fit to the BR's of CF PP modes gives (in units of 10^{-6}):

$$T = 3.113 \pm 0.011 \quad \text{— real by convention}$$

such magnitudes and strong phases signify that amplitudes other than T all receive significant nonfactorizable, long-distance FSI's
 more on this later

$$\text{— } C = (2.767 \pm 0.029)e^{-i(151.3 \pm 0.3)^\circ}$$

$$\text{— } E = (1.48 \pm 0.04)e^{i(120.9 \pm 0.4)^\circ}$$

$$\text{— } A = (0.55 \pm 0.03)e^{i(23+7)^\circ}$$

cf. B decays

Cheng and CWC 2019
 with slight updates in
 Cheng and CWC 2024

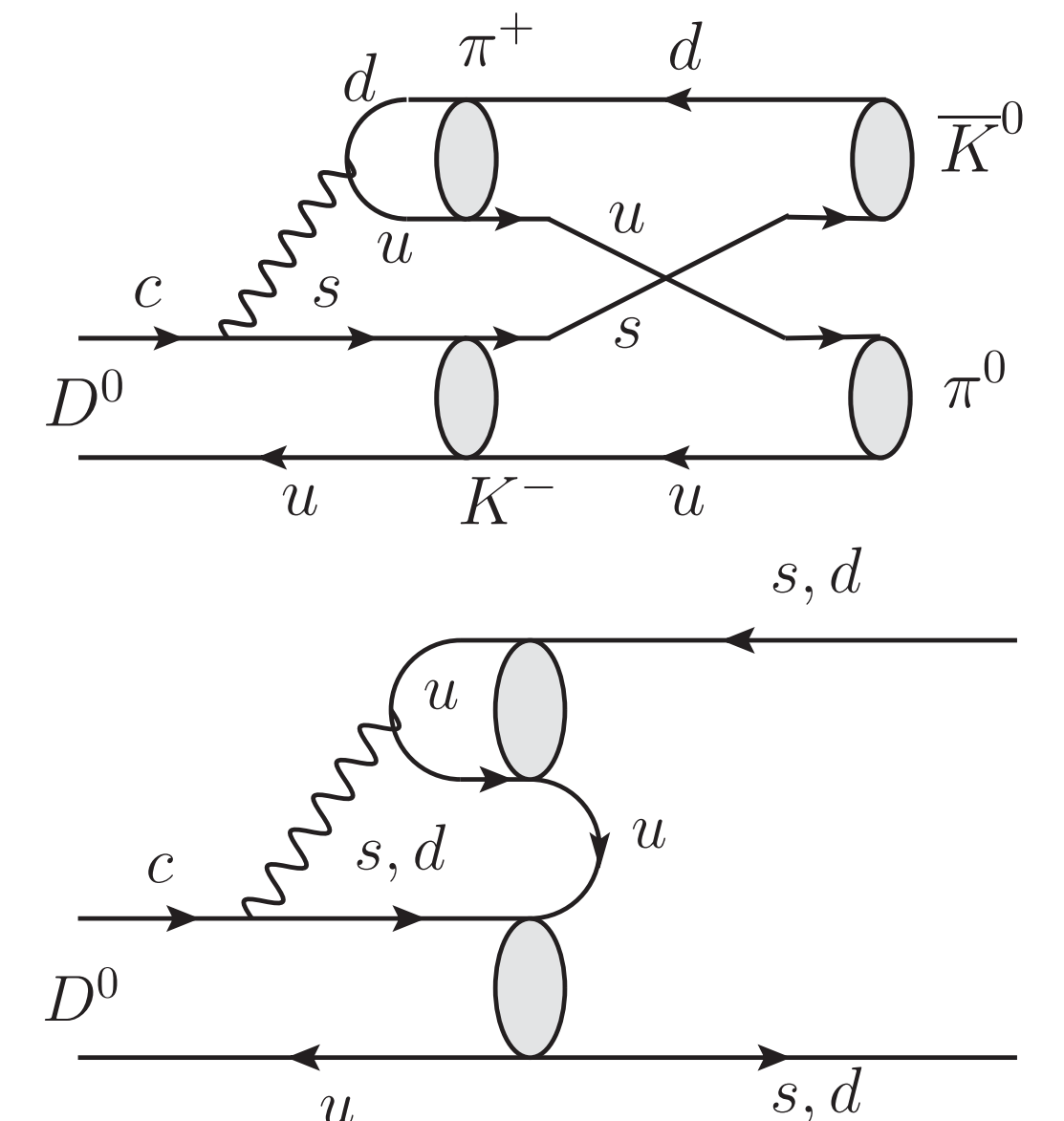
large strong phases

- For example, the effective Wilson coefficients for the T and C amplitudes are given by:

$$\text{extracted from data — } a_1(\bar{K}\pi) \approx 1.22 \quad \text{and} \quad a_2(\bar{K}\pi) \approx 0.82e^{-i(151)^\circ}$$

$$\text{naive factorization — } a_1 \simeq 1.09 \quad \text{and} \quad a_2 \simeq -0.11$$

- Both C and E can be enhanced by **rescattering** from T .



Cheng, CWC 2010

The $D \rightarrow \pi^+ \pi^-$ and $K^+ K^-$ Decays

- These two SCS decay modes are closely related:

$$A_{\pi^+ \pi^-} = \frac{1}{2}(\lambda_d - \lambda_s)(T + E + \Delta P)_{\pi\pi} - \frac{1}{2}\lambda_b(T + E + \Sigma P)_{\pi\pi}$$

opposite in sign
 \Rightarrow opposite in CPA

$$\Rightarrow \lambda_d(T + E) - \lambda_b \Sigma P \quad [\text{SU}(3) \text{ limit}]$$

$$A_{K^+ K^-} = \frac{1}{2}(\lambda_s - \lambda_d)(T + E - \Delta P)_{KK} - \frac{1}{2}\lambda_b(T + E + \Sigma P)_{KK}$$

$$\Rightarrow \lambda_s(T + E) - \lambda_b \Sigma P \quad [\text{SU}(3) \text{ limit}]$$

where the penguin amplitudes can be safely ignored in BR calculations, and

$$\Sigma P = (P + PE + PA)_d + (P + PE + PA)_s \quad \text{— sum of } d\text{- and } s\text{- penguins}$$

$$\Delta P = (P + PE + PA)_d - (P + PE + PA)_s \quad \text{— difference between } d\text{- and } s\text{- penguins}$$

$$\lambda_q = V_{cq}^* V_{uq}$$

the quark involved in the penguin loop

- In the SU(3) limit, their amplitudes are the **same** in magnitude and their CPA's are **opposite**. \Rightarrow **sum rule**: the sum of individual CPA's vanishes

Improved Sum Rule and Data

- In the U-spin limit, there is an **improved sum rule**:

$$\frac{a_{\text{CP}}^{\text{dir}}(D^0 \rightarrow \pi^+ \pi^-)}{a_{\text{CP}}^{\text{dir}}(D^0 \rightarrow K^+ K^-)} = -\frac{\Gamma(D^0 \rightarrow K^+ K^-)}{\Gamma(D^0 \rightarrow \pi^+ \pi^-)} < 0$$

Grossman, Kagan, Nir 2007
Pirtskhalava, Uttayarat 2012
Grossman, Robinson 2013

while data show that it is **broken**:

$$3.01_{-5.95}^{+0.95} \neq -2.81 \pm 0.06 !$$

LHCb 2023
Schacht 2023

- The latest HFLAV data,

$$a_{\text{CP}}^{\text{dir}}(D^0 \rightarrow \pi^+ \pi^-) = (2.30 \pm 0.59) \times 10^{-3}$$

$$a_{\text{CP}}^{\text{dir}}(D^0 \rightarrow K^+ K^-) = (0.44 \pm 0.54) \times 10^{-3}$$

HFLAV 2023

also supports the **same-sign** CPA's.

- Such a disagreement is **beyond** the naive SU(3) symmetry breaking of ~30%.

Large SU(3) Breaking

- For a long time, the BR's of $D \rightarrow \pi^+ \pi^-$, $K^+ K^-$ are known to deviate significantly from naive expectations: with negligible penguin amplitudes, the two modes have **identical decay strength**, but with **different phase spaces**.

⇒ expect $\mathcal{B}(\pi^+ \pi^-) > \mathcal{B}(K^+ K^-)$

- Empirically, however, the ratio of their decay rates

$$\frac{\Gamma(K^+ K^-)}{\Gamma(\pi^+ \pi^-)} \simeq 2.8$$

is noticeably **larger than 1** in the SU(3) limit (neglecting phase space effects).

- It has been argued that such a ratio can be explained by SU(3) breaking on the amplitude of the order of

$$\varepsilon = \frac{m_s - m_d}{\Lambda_{\text{QCD}}} \sim 0.3$$

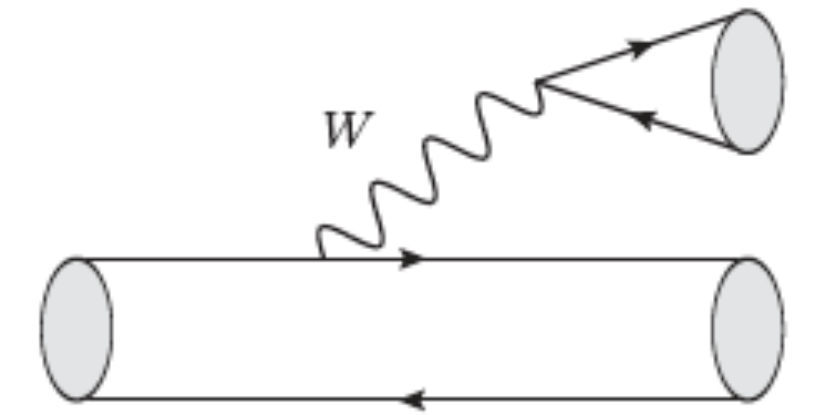
Schacht 2023

Large SU(3) Breaking

- SU(3) breaking in T :

$$\frac{T(K^+K^-)}{T(\pi^+\pi^-)} \simeq \frac{f_K}{f_\pi} \frac{F_+^{DK}(m_K^2)}{F_+^{D\pi}(m_\pi^2)} \simeq 1.32$$

⇒ however, not the complete story



Large SU(3) Breaking

- SU(3) breaking in T :

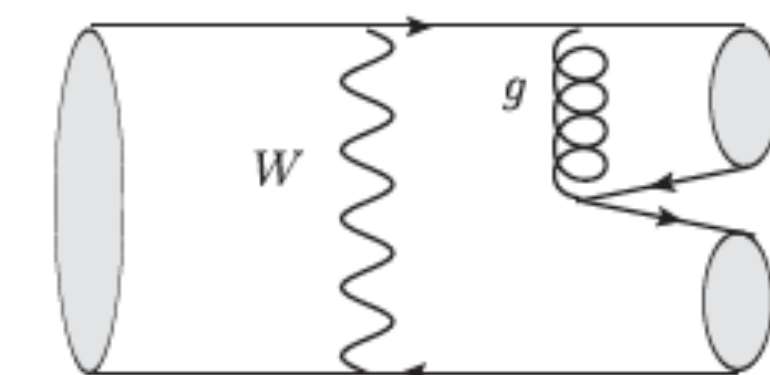
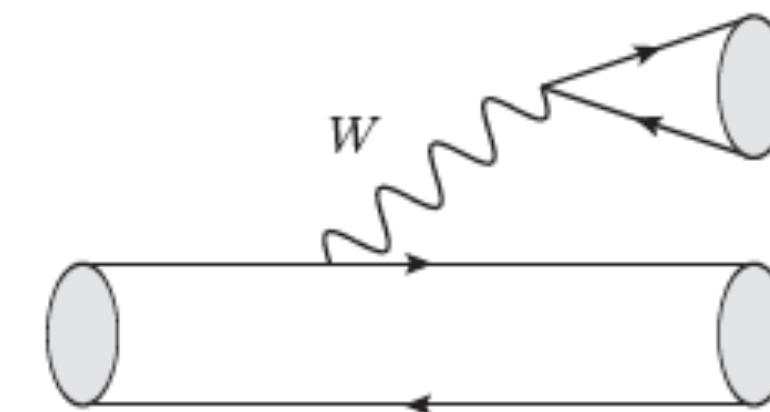
$$\frac{T(K^+ K^-)}{T(\pi^+ \pi^-)} \simeq \frac{f_K}{f_\pi} \frac{F_+^{DK}(m_K^2)}{F_+^{D\pi}(m_\pi^2)} \simeq 1.32$$

⇒ however, not the complete story

- SU(3) breaking in E :

vanishing in SU(3) limit — $A(D \rightarrow K^0 \overline{K}^0) = \lambda_d (E_d + 2PA_d) + \lambda_s (E_s + 2PA_s)$

| opposite sign between them |
| diagrams of $c\bar{u} \rightarrow q\bar{q}$ ($q = d, s$) |



⇒ needs different E_d and E_s to explain the nonzero rate:

$$\begin{cases} \text{I:} & E_d = 1.10e^{i15.1^\circ} E, & E_s = 0.62e^{-i19.7^\circ} E \\ \text{II:} & E_d = 1.10e^{i15.1^\circ} E, & E_s = 1.42e^{-i13.5^\circ} E \end{cases}$$

— two possible solutions for symmetry breaking

Large SU(3) Breaking

- SU(3) breaking in T :

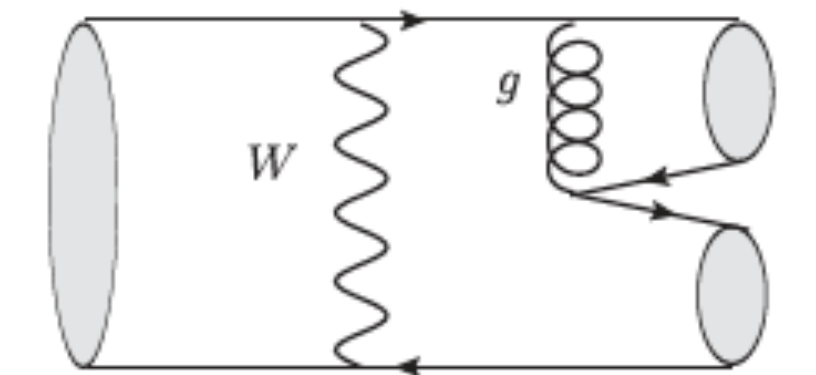
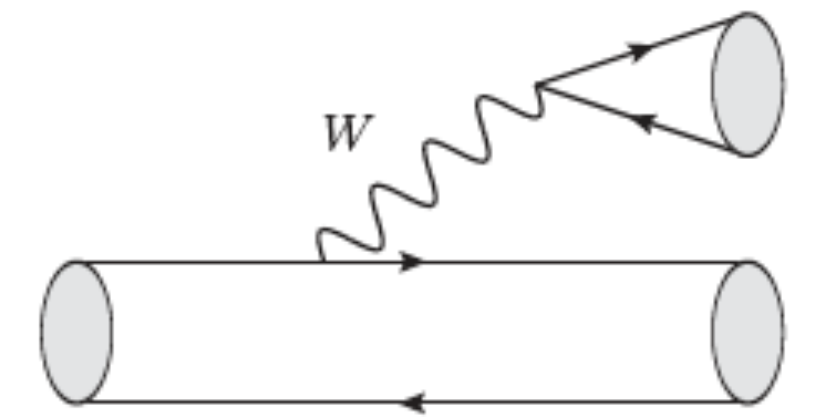
$$\frac{T(K^+K^-)}{T(\pi^+\pi^-)} \simeq \frac{f_K}{f_\pi} \frac{F_+^{DK}(m_K^2)}{F_+^{D\pi}(m_\pi^2)} \simeq 1.32$$

⇒ however, not the complete story

- SU(3) breaking in E :

vanishing in SU(3) limit — $A(D \rightarrow K^0 \overline{K^0}) = \lambda_d (E_d + 2PA_d) + \lambda_s (E_s + 2PA_s)$

opposite sign between them
| |
diagrams of $c\bar{u} \rightarrow q\bar{q}$ ($q = d, s$)



⇒ needs different E_d and E_s to explain the nonzero rate:

$$\begin{cases} \text{I: } E_d = 1.10e^{i15.1^\circ} E, & E_s = 0.62e^{-i19.7^\circ} E \\ \text{II: } E_d = 1.10e^{i15.1^\circ} E, & E_s = 1.42e^{-i13.5^\circ} E \end{cases}$$

— two possible solutions for symmetry breaking

- Agglutination of these effects leads to apparently large SU(3) breaking in the observed rates of K^+K^- , $\pi^+\pi^-$, $\pi^0\pi^0$ and $K^0\overline{K^0}$.

Results

- Our fit results are (in units of 10^{-3})

Cheng, CWC 2019

Decay mode	$\pi^+\pi^-$	$\pi^0\pi^0$	K^+K^-	$K_S K_S$
$\mathcal{B}_{\text{SU}(3)}$	2.28 ± 0.02	1.50 ± 0.03	1.91 ± 0.02	0
$\mathcal{B}_{\text{SU}(3)}$	1.47 ± 0.02	0.82 ± 0.02	4.03 ± 0.03	0.141 ± 0.007
\mathcal{B}_{exp}	1.455 ± 0.024	0.826 ± 0.025	4.08 ± 0.06	0.141 ± 0.005

- With **naive QCDF** and **tree-level matrix elements using LCSR**, the perturbation approach gives

$$\mathcal{B}(\pi^+\pi^-)|_{\text{LCSR}} = (1.40^{+1.53}_{-1.06}) \times 10^{-3}$$

$$\mathcal{B}(K^+K^-)|_{\text{LCSR}} = (3.67^{+3.90}_{-2.69}) \times 10^{-3}$$

Lenz, Piscopo, Rusov 2024

also in agreement with data, though with large theory uncertainties coming from conservative estimates of missing contributions.

- The branching ratio puzzle can be resolved in either approach.

Tree-level CPV

- Direct CPA's in hadronic charm decays can occur even **at the tree level**, through the interference between T and C , C and E , or even between E 's. Chau, Cheng 1984
Cheng, CWC 2012

- As an example, $A(D \rightarrow K^0 \bar{K}^0) = \lambda_d E_d + \lambda_s E_s$ (vanishing in the SU(3) limit) when neglecting the PA amplitudes, leading to the **prediction**

$$a_{\text{CP}}^{\text{dir}}(K_S K_S) = \frac{2 \text{Im}(\lambda_d \lambda_s^*) \text{Im}(E_d^* E_s)}{|\lambda_d|^2 |E_d - E_s|^2} = 1.3 \times 10^{-3} \frac{|E_d E_s|}{|E_d - E_s|^2} \sin \delta_{ds}$$

$$= \begin{cases} -1.05 \times 10^{-3} \\ -1.99 \times 10^{-3} \end{cases} \quad \begin{array}{l} \text{from the two possible solutions of } E_{d,s}; \\ \text{— a precise measurement of it will resolve} \\ \text{the ambiguity} \end{array}$$

which are virtually unchanged when PA contributions are also included.

- In contrast, the factorization-assisted topological-amplitude (FAT) approach predicts 1.11×10^{-3} , **opposite in sign**. Li, Lü, Yu 2012
- Latest HFLAV gives $a_{\text{CP}}^{\text{dir}}(K_S K_S) = -0.019 \pm 0.010$. HFLAV 2023

Penguin-induced CPV

- Direct CPV does not occur at the tree level in $D^0 \rightarrow K^+K^-$ and $D^0 \rightarrow \pi^+\pi^-$.
 ■■■ CPA arises from the interference between tree and penguin amplitudes

$$\Delta a_{\text{CP}}^{\text{dir}} = -1.30 \times 10^{-3} \left(\left| \frac{P_d + PE_d + PA_d}{T + E - \Delta P} \right|_{KK} \sin \delta_{KK} + \left| \frac{P_s + PE_s + PA_s}{T + E + \Delta P} \right|_{\pi\pi} \sin \delta_{\pi\pi} \right)$$

negligible
strong phases of the numerator relative to the denominator

- For the QCD penguin amplitudes, people employ QCDF, pQCD and LCSR:

$$\left(\frac{P}{T} \right)_{\pi\pi}^{\text{QCDF}} \approx 0.23e^{-i150^\circ} \quad \left(\frac{P}{T} \right)_{KK}^{\text{QCDF}} \approx 0.22e^{-i150^\circ} \quad \text{Cheng, CWC 2019}$$

$$\left(\frac{P}{T} \right)_{\pi\pi}^{\text{pQCD}} \approx 0.30e^{i110^\circ} \quad \left(\frac{P}{T} \right)_{KK}^{\text{pQCD}} \approx 0.24e^{i110^\circ} \quad \text{Li, Lü, Yu 2012}$$

a factor of ~3 smaller than above —

$$\left| \frac{P}{T} \right|_{\pi\pi}^{\text{LCSR}} = 0.089^{+0.042}_{-0.037} \quad \left| \frac{P}{T} \right|_{KK}^{\text{LCSR}} = 0.066^{+0.031}_{-0.029} \quad \text{Khodjamirian, Petrov 2017}$$

Lenz, Piscopo, Rusov 2024

showing some difference between LCSR and QCD-inspired approaches.

Estimates of $\Delta a_{\text{CP}}^{\text{dir}}$ Without FSI's

- The CPA difference is measured to be

$$\Delta a_{\text{CP}}^{\text{dir}} \Big|_{\text{exp}} = (-15.7 \pm 2.9) \times 10^{-4}$$

LHCb 2019

- Taking the above-mentioned $|P/T|$ ratios from LCSR and varying strong phases, one obtains an upper bound of

$$|\Delta a_{\text{CP}}^{\text{dir}}| \leq 2.4 \times 10^{-4}$$

Lenz, Piscopo, Rusov 2024

6 times smaller than the above measurement.

▮▮▮ violation of quark-hadron duality used in the calculation is hard to estimate

- Using QCDF for penguin amplitudes, we also have

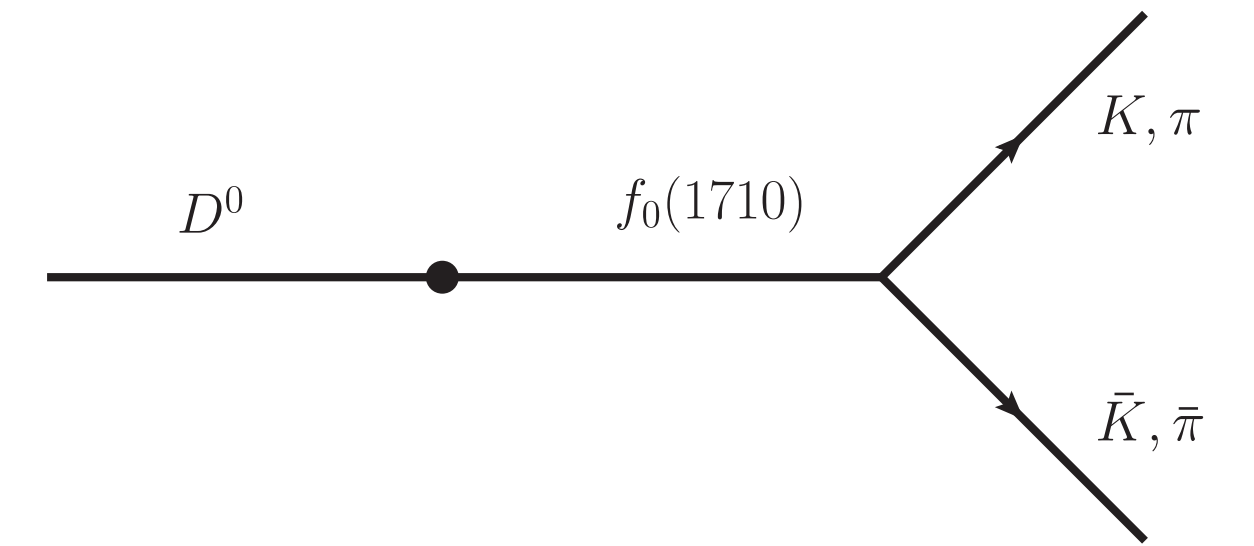
$$|\Delta a_{\text{CP}}^{\text{dir}}| \sim \mathcal{O}(10^{-4})$$

Cheng, CWC 2019

after further including PE and PA amplitudes, making the penguin strong phase even **closer to 180°** .

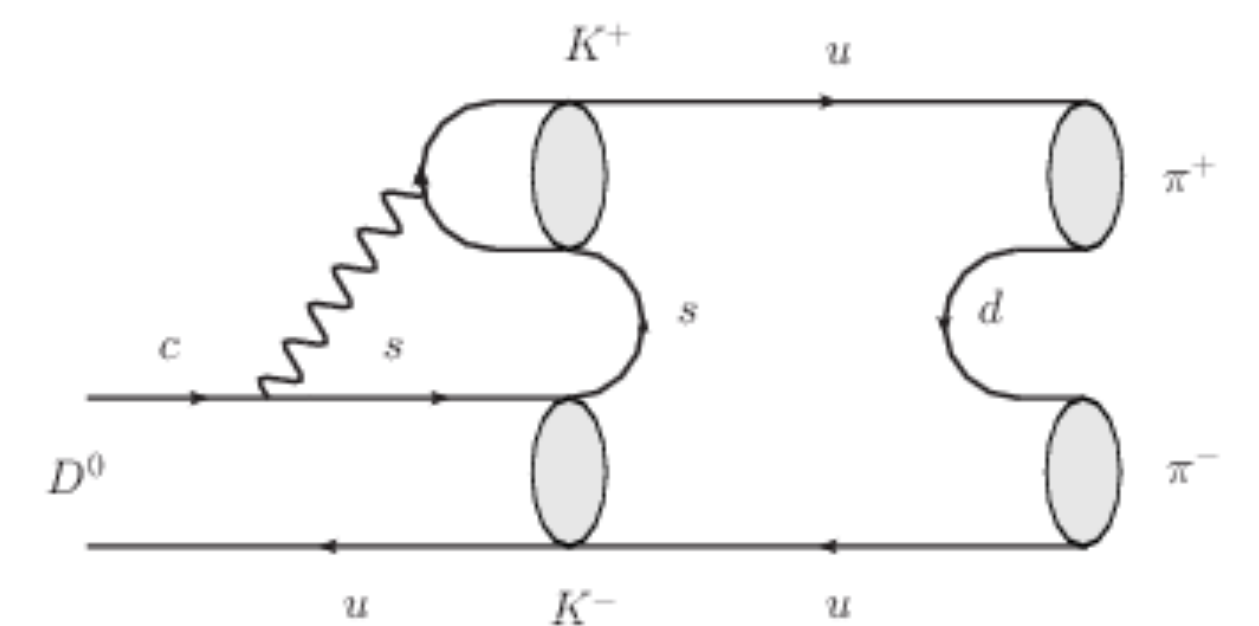
Final-State Interactions

- An isospin amplitude analysis incorporates **nearby scalar resonances** of $f_0(1710)$ and/or $f_0(1790)$ claims to be able to explain the $\Delta a_{\text{CP}}^{\text{dir}}$ data.
 - ▮ need more precise experimental information on the BR's of such scalars to KK and $\pi\pi$ to verify the dynamical mechanism



Cheng, CWC 2010
Schacht, Soni 2022

- Although short-distance PE and PA amplitudes are negligibly small ($|PE/T| \sim 0.04$ and $|PA/T| \sim 0.02$), **large long-distance contributions** to $P + PE$ can possibly arise from $D^0 \rightarrow K^+ K^-$ followed by a **resonance-like final-state interaction (FSI) rescattering**.



topologically $P + PE$ -like

Cheng, CWC 2013

- It is thus conceivable to have $(P + PE)^{\text{LD}} \sim E$, in both strength and strong phase. ▮ take $(P + PE)_{d,s}^{\text{LD}} \approx (1.48 \pm 0.30)e^{i(120.9 \pm 30.0)^\circ}$

$\Delta a_{\text{CP}}^{\text{dir}}$ in Symmetry-based Approach

Cheng, CWC 2019

- Due to mainly the enhancement of $(PE)_{d,s}^{\text{LD}}$, we have

$$\left(\frac{P_s + PE_s + PA_s + PE_s^{\text{LD}}}{T + E^d + \Delta P} \right)_{\pi\pi} = 0.77e^{i114^\circ} \text{ — closer to } 90^\circ$$

$$\left(\frac{P_d + PE_d + PA_d + PE_d^{\text{LD}}}{T + E^s - \Delta P} \right)_{KK} = \begin{cases} 0.45e^{i117^\circ} & \text{solution I} \\ 0.45e^{i110^\circ} & \text{solution II} \end{cases}$$

Note that no attempt has been made to fit CPA's!

not so huge enhancement in magnitudes in comparison with QCDF calculation

leading to the prediction

$$a_{\text{CP}}^{\text{dir}}(\pi^+\pi^-) = (0.80 \pm 0.22) \times 10^{-3}$$

$$a_{\text{CP}}^{\text{dir}}(K^+K^-) = \begin{cases} (-0.33 \pm 0.14) \times 10^{-3} & \text{Solution I} \\ (-0.44 \pm 0.12) \times 10^{-3} & \text{Solution II} \end{cases}$$

$$\Rightarrow \Delta a_{\text{CP}}^{\text{dir}} = \begin{cases} (-1.14 \pm 0.26) \times 10^{-3} & \text{Solution I} \\ (-1.25 \pm 0.25) \times 10^{-3} & \text{Solution II} \end{cases}$$

— still predict opposite-sign CPA's

More About Final-State Interactions

- Based upon general arguments of **CPT invariance** and considering the ***S*-wave *S*-matrix** for the rescattering of the two coupled channels of $\pi^+\pi^-$ and K^+K^- purely **within SM**, it is derived that

Bediaga, Frederico, Magalhães 2023

$$\sum_{f=\pi\pi, KK} \left(|\mathcal{A}_{D^0 \rightarrow f}|^2 - |\mathcal{A}_{\bar{D}^0 \rightarrow f}|^2 \right) = 0 \quad \text{— due to CPT invariance for the two-channel scattering}$$

$$a_{\text{CP}}^{\text{dir}}(\pi\pi) = -\frac{\Delta a_{\text{CP}}^{\text{dir}} \mathcal{B}(D^0 \rightarrow K^+K^-)}{\sum \mathcal{B}} = (1.135 \pm 0.021) \times 10^{-3}$$

$$a_{\text{CP}}^{\text{dir}}(KK) = \frac{\Delta a_{\text{CP}}^{\text{dir}} \mathcal{B}(D^0 \rightarrow \pi^+\pi^-)}{\sum \mathcal{B}} = -(0.405 \pm 0.077) \times 10^{-3}$$

also predicting opposite CPA's

$$\text{where } \sum \mathcal{B} \equiv \mathcal{B}(D^0 \rightarrow K^+K^-) + \mathcal{B}(D^0 \rightarrow \pi^+\pi^-)$$

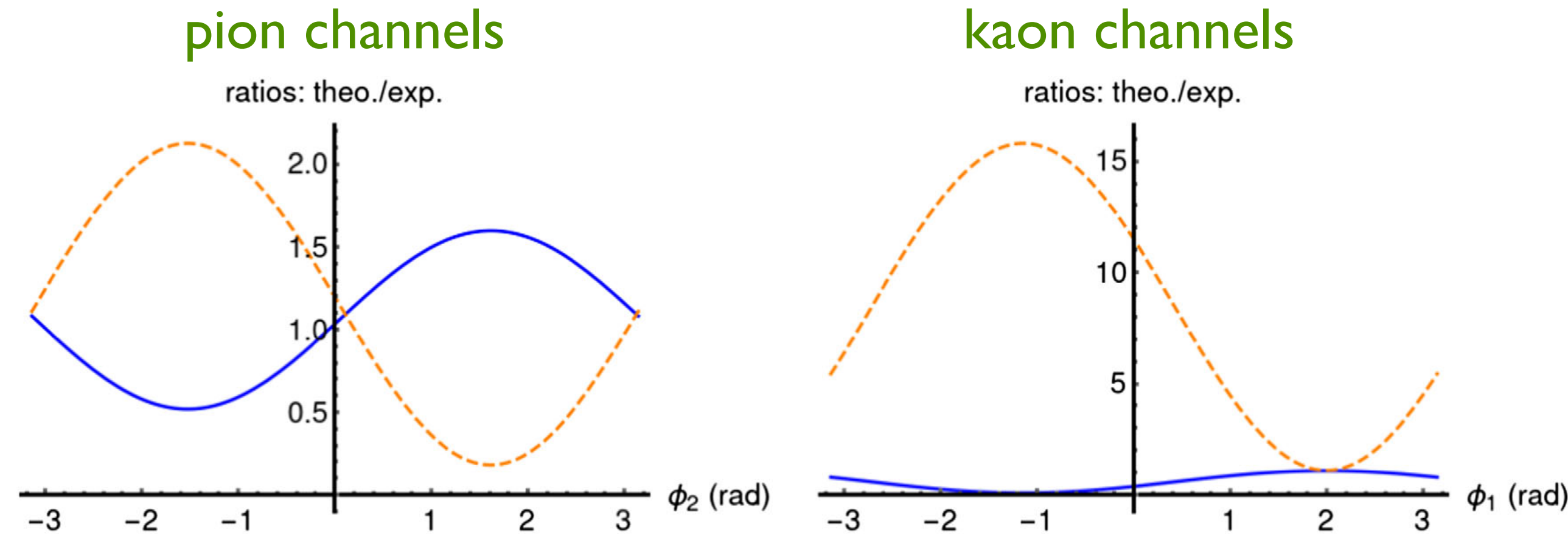
$$\Delta a_{\text{CP}}^{\text{dir}} = (-1.31 \pm 0.20) \times 10^{-3} \quad \text{— using a particular set of parameter and strong phases}$$

More About Final-State Interactions

- Although the importance of rescattering effects has been recognized, it is argued that a full picture should be obtained by employing **dispersive relations**.

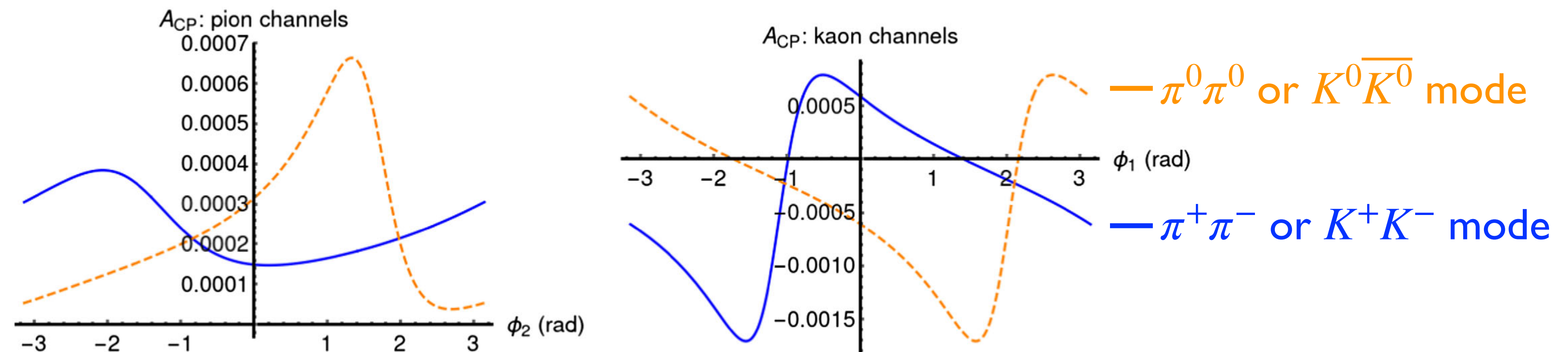
Pich, Solomonidi, Silva 2023

ratios of theory and experimental BR's



Only pion and kaon pairs are included in the analysis. There is a plan to include further inelasticities.

predicted CPA's are much below the experimental values



- Rescattering effects turn out producing **insufficient** enhancement for CPA's.

Predictions / Data on BR's / CPA's of SCS PP Decays

Cheng, CWC 2019

	Mode	\mathcal{B}		a_{CP}^{dir}		
		ours	exp	ours	Buccella+ 2019	HFLAV
$D^0 \rightarrow$	$\pi^+ \pi^-$	1.47 ± 0.02	1.455 ± 0.024	0.80 ± 0.22	$1.17 \pm 0.20/1.18 \pm 0.20$	2.30 ± 0.59
	$\pi^0 \pi^0$	0.82 ± 0.02	0.826 ± 0.025	0.82 ± 0.30	$0.04 \pm 0.09/0.79 \pm 0.10$	-0.3 ± 6.4
	$\pi^0 \eta$	0.92 ± 0.02	0.63 ± 0.06	-0.05 ± 0.28		
	$\pi^0 \eta'$	1.36 ± 0.03	0.92 ± 0.10	-0.15 ± 0.17		
	$\eta\eta$	1.82 ± 0.04	2.11 ± 0.19	-0.52 ± 0.07		
		2.11 ± 0.04		-0.65 ± 0.07		
	$\eta\eta'$	0.69 ± 0.03	1.01 ± 0.19	0.29 ± 0.21		
		1.63 ± 0.08		0.22 ± 0.15		
	$K^+ K^-$	4.03 ± 0.03	4.08 ± 0.06	-0.33 ± 0.14	$-0.47 \pm 0.08/ -0.46 \pm 0.08$	0.44 ± 0.54
		4.05 ± 0.05		-0.44 ± 0.12		
D^+	$K_S K_S$	0.141 ± 0.007	0.141 ± 0.005	-1.05	$0.43 \pm 0.07/0.38 \pm 0.07$	-19 ± 10
		0.141 ± 0.007		-1.99		
$D^+ \rightarrow$	$\pi^+ \pi^0$	0.93 ± 0.02	1.247 ± 0.033	0		
	$\pi^+ \eta$	4.08 ± 0.16	3.77 ± 0.09	-0.63 ± 0.23		
	$\pi^+ \eta'$	4.69 ± 0.08	4.97 ± 0.19	0.11 ± 0.18		
	$K^+ K_S$	4.25 ± 0.10	3.04 ± 0.09	-0.30 ± 0.18	$-0.40 \pm 0.07/ -0.26 \pm 0.05$	
$D_s^+ \rightarrow$	$\pi^+ K_S$	1.27 ± 0.04	1.22 ± 0.06	0.42 ± 0.24	$-0.40 \pm 0.07/ -0.36 \pm 0.07$	
	$\pi^0 K^+$	0.56 ± 0.02	0.63 ± 0.21	0.91 ± 0.27	$0.48 \pm 0.06/ -0.03 \pm 0.04$	
	$K^+ \eta$	0.86 ± 0.03	1.77 ± 0.35	-0.81 ± 0.08		
	$K^+ \eta'$	1.49 ± 0.08	1.8 ± 0.6	0.07 ± 0.25		

all in units of 10^{-3}

Predictions / Data on BR's / CPA's of SCS PP Decays

Cheng, CWC 2019

	Mode	\mathcal{B}		a_{CP}^{dir}		
		ours	exp	ours	Buccella+ 2019	HFLAV
$D^0 \rightarrow$	$\pi^+ \pi^-$	1.47 ± 0.02	1.455 ± 0.024	0.80 ± 0.22	$1.17 \pm 0.20 / 1.18 \pm 0.20$	2.30 ± 0.59
	$\pi^0 \pi^0$	0.82 ± 0.02	0.826 ± 0.025	0.82 ± 0.30	$0.04 \pm 0.09 / 0.79 \pm 0.10$	-0.3 ± 6.4
	$\pi^0 \eta$	0.92 ± 0.02	0.63 ± 0.06	-0.05 ± 0.28		
	$\pi^0 \eta'$	1.36 ± 0.03	0.92 ± 0.10	-0.15 ± 0.17		
	$\eta\eta$	1.82 ± 0.04	2.11 ± 0.19	-0.52 ± 0.07		
		2.11 ± 0.04		-0.65 ± 0.07		
	$\eta\eta'$	0.69 ± 0.03	1.01 ± 0.19	0.29 ± 0.21		
		1.63 ± 0.08		0.22 ± 0.15		
	$K^+ K^-$	4.03 ± 0.03	4.08 ± 0.06	-0.33 ± 0.14	$-0.47 \pm 0.08 / -0.46 \pm 0.08$	0.44 ± 0.54
		4.05 ± 0.05		-0.44 ± 0.12		
	$K_S K_S$	0.141 ± 0.007	0.141 ± 0.005	-1.05	$0.43 \pm 0.07 / 0.38 \pm 0.07$	-19 ± 10
		0.141 ± 0.007		-1.99		
$D^+ \rightarrow$	$\pi^+ \pi^0$	0.93 ± 0.02	1.247 ± 0.033	0		
	$\pi^+ \eta$	4.08 ± 0.16	3.77 ± 0.09	-0.63 ± 0.23		
	$\pi^+ \eta'$	4.69 ± 0.08	4.97 ± 0.19	0.11 ± 0.18		
	$K^+ K_S$	4.25 ± 0.10	3.04 ± 0.09	-0.30 ± 0.18	$-0.40 \pm 0.07 / -0.26 \pm 0.05$	
$D_s^+ \rightarrow$	$\pi^+ K_S$	1.27 ± 0.04	1.22 ± 0.06	0.42 ± 0.24	$-0.40 \pm 0.07 / -0.36 \pm 0.07$	
	$\pi^0 K^+$	0.56 ± 0.02	0.63 ± 0.21	0.91 ± 0.27	$0.48 \pm 0.06 / -0.03 \pm 0.04$	
	$K^+ \eta$	0.86 ± 0.03	1.77 ± 0.35	-0.81 ± 0.08		
	$K^+ \eta'$	1.49 ± 0.08	1.8 ± 0.6	0.07 ± 0.25		

modes of interest,
with sufficiently large
BR's and CPA's.

all in units of 10^{-3}

Predictions / Data on BR's / CPA's of SCS PP Decays

Cheng, CWC 2019

	Mode	\mathcal{B}		a_{CP}^{dir}		
		ours	exp	ours	Buccella+ 2019	HFLAV
$D^0 \rightarrow$	$\pi^+ \pi^-$	1.47 ± 0.02	1.455 ± 0.024	0.80 ± 0.22	$1.17 \pm 0.20 / 1.18 \pm 0.20$	2.30 ± 0.59
	$\pi^0 \pi^0$	0.82 ± 0.02	0.826 ± 0.025	0.82 ± 0.30	$0.04 \pm 0.09 / 0.79 \pm 0.10$	-0.3 ± 6.4
	$\pi^0 \eta$	0.92 ± 0.02	0.63 ± 0.06	-0.05 ± 0.28		
	$\pi^0 \eta'$	1.36 ± 0.03	0.92 ± 0.10	-0.15 ± 0.17		
	$\eta\eta$	1.82 ± 0.04	2.11 ± 0.19	-0.52 ± 0.07		
		2.11 ± 0.04		-0.65 ± 0.07		
	$\eta\eta'$	0.69 ± 0.03	1.01 ± 0.19	0.29 ± 0.21		
		1.63 ± 0.08		0.22 ± 0.15		
	$K^+ K^-$	4.03 ± 0.03	4.08 ± 0.06	-0.33 ± 0.14	$-0.47 \pm 0.08 / -0.46 \pm 0.08$	0.44 ± 0.54
		4.05 ± 0.05		-0.44 ± 0.12		
	$K_S K_S$	0.141 ± 0.007	0.141 ± 0.005	-1.05	$0.43 \pm 0.07 / 0.38 \pm 0.07$	-19 ± 10
		0.141 ± 0.007		-1.99		
$D^+ \rightarrow$	$\pi^+ \pi^0$	0.93 ± 0.02	1.247 ± 0.033	0		
	$\pi^+ \eta$	4.08 ± 0.16	3.77 ± 0.09	-0.63 ± 0.23		
	$\pi^+ \eta'$	4.69 ± 0.08	4.97 ± 0.19	0.11 ± 0.18		
	$K^+ K_S$	4.25 ± 0.10	3.04 ± 0.09	-0.30 ± 0.18	$-0.40 \pm 0.07 / -0.26 \pm 0.05$	
$D_s^+ \rightarrow$	$\pi^+ K_S$	1.27 ± 0.04	1.22 ± 0.06	0.42 ± 0.24	$-0.40 \pm 0.07 / -0.36 \pm 0.07$	
	$\pi^0 K^+$	0.56 ± 0.02	0.63 ± 0.21	0.91 ± 0.27	$0.48 \pm 0.06 / -0.03 \pm 0.04$	
	$K^+ \eta$	0.86 ± 0.03	1.77 ± 0.35	-0.81 ± 0.08		
	$K^+ \eta'$	1.49 ± 0.08	1.8 ± 0.6	0.07 ± 0.25		

modes of interest, with sufficiently large BR's and CPA's.

predict $\Delta a_{CP}^{\text{dir}}(K^+ K^- - \pi^+ \pi^-)$ to be $(-1.14 \pm 0.26) \times 10^{-3}$ or $(-1.25 \pm 0.25) \times 10^{-3}$

all in units of 10^{-3}

Topological Diagrams for $D \rightarrow VP$ Decays

- In the case of $D \rightarrow VP$ decays, the spectator quark in the D meson may end up in P or V meson in the final state. Though of the same flavor topology, these two types of diagrams have **no relation a priori** and should be distinguished.
 - **Less significant** SU(3) breaking for $T_{V,P}$ and $C_{P,V}$. For example,

$$\frac{|T_V + E_P|_{\pi^+\rho^-}}{|T_V + E_P|_{K^+K^{*-}}} \simeq 1.08 \quad \frac{|T_P + E_V|_{\pi^-\rho^+}}{|T_P + E_V|_{K^-K^{*+}}} \simeq 0.91$$
 - $A_{V,P}$ **roughly in phase** for small $\mathcal{B}(\pi^+\rho)$ and large $\mathcal{B}(\pi^+\omega)$ of D_s^+ .
 - $C_{V,P}$ **roughly in phase** for small $\mathcal{B}(\pi^0\omega)$, sizable $\mathcal{B}(\eta\omega)$, and large $\mathcal{B}(\pi^0\rho^0)$ of D^0 .
- Analogous to the PP sector, **SU(3) breaking** is required in the d, s -type $E_{V,P}$ in order to explain nonzero rates of $D^0 \rightarrow K^0\overline{K^{*0}}$ and $\overline{K^0}K^{*0}$.

Predictions / Data on BR's / CPA's of SCS *VP* Decays

		\mathcal{B}			$a_{\text{CP}}^{\text{dir}}$		
	Mode	ours	Qin+ 2014	exp	ours	Qin+ 2014	HFLAV
$D^0 \rightarrow$	$\pi^+ \rho^-$	5.12 ± 0.29	4.74/4.66	5.15 ± 0.25	0.77 ± 0.22	-0.03	
	$\pi^- \rho^+$	10.21 ± 0.91	10.2/10.0	10.1 ± 0.4	-0.14 ± 0.04	-0.01	
	$\pi^0 \rho^0$	3.90 ± 0.26	3.55/3.83	3.86 ± 0.23	0.37 ± 0.15	-0.03	
	$K^+ K^{*-}$	1.68 ± 0.11	1.72/1.73	1.65 ± 0.11	-0.75 ± 0.37	-0.01	
	$K^- K^{*+}$	4.43 ± 0.31	4.37/4.37	4.56 ± 0.21	0.15 ± 0.04	0	
	$K^0 \bar{K}^{*0}$	0.27 ± 0.06	1.1/1.1	0.246 ± 0.048	-0.15 ± 0.21	-0.7	
	$\bar{K}^0 K^{*0}$	0.32 ± 0.09	1.1/1.1	0.336 ± 0.063	-0.34 ± 0.16	-0.7	
	$\pi^0 \omega$	0.12 ± 0.05	0.85/0.18	0.117 ± 0.035	-2.14 ± 0.95	0.02	
	$\pi^0 \phi$	1.22 ± 0.04	1.11/1.11	1.20 ± 0.04	0	-0.0002	
	$\eta \omega$	2.25 ± 0.14	2.4/2.0	1.98 ± 0.18	-0.38 ± 0.10	-0.1	
	$\eta' \omega$	0.01 ± 0.00	0.04/0.02	...	0.96 ± 0.66	2.2	
	$\eta \phi$	0.16 ± 0.02	0.19/0.18	0.167 ± 0.034	0	0.003	$-19 \pm 44 \pm 6$
	$\eta \rho^0$	0.59 ± 0.07	0.54/0.45	...	0.10 ± 0.30	1.0	
	$\eta' \rho^0$	0.06 ± 0.01	0.21/0.27	...	0.16 ± 0.22	-0.1	
$D^+ \rightarrow$	$\pi^+ \rho^0$	0.61 ± 0.10	0.42/0.58	0.83 ± 0.15	2.20 ± 1.38	0.5	
	$\pi^0 \rho^+$	4.53 ± 0.64	2.7/2.5	...	0.49 ± 0.37	0.2	
	$\pi^+ \omega$	0.26 ± 0.07	0.95/0.80	0.28 ± 0.06	0.74 ± 2.03	-0.05	
	$\pi^+ \phi$	6.29 ± 0.20	5.65/5.65	5.68 ± 0.11	0	-0.0001	
	$\eta \rho^+$	1.02 ± 0.34	0.7/2.2	...	1.78 ± 0.69	-0.6	
	$\eta' \rho^+$	1.03 ± 0.11	0.7/0.8	...	0.08 ± 0.11	0.5	
	$K^+ \bar{K}^{*0}$	3.82 ± 0.25	3.61/3.60	$3.83_{-0.21}^{+0.14}$	-1.06 ± 0.30	0.2	
$D_s^+ \rightarrow$	$\bar{K} K^{*+}$	9.80 ± 0.41	11/11	34 ± 16	0.10 ± 0.04	0.04	
	$\pi^+ K^{*0}$	3.65 ± 0.24	2.52/2.35	2.13 ± 0.36	1.05 ± 0.30	-0.1	
	$\pi^0 K^{*+}$	1.02 ± 0.07	0.8/1.0	...	1.15 ± 0.40	-0.2	
	$K^+ \rho^0$	2.10 ± 0.10	1.9/2.5	2.5 ± 0.4	-0.08 ± 0.07	0.3	
	$K^0 \rho^+$	11.47 ± 0.48	9.1/9.6	...	-0.08 ± 0.04	0.3	
	ηK^{*+}	0.64 ± 0.20	0.2/0.2	...	0.10 ± 0.48	1.1	
	$\eta' K^{*+}$	0.33 ± 0.02	0.2/0.2	...	-0.12 ± 0.13	-0.5	
	$K^+ \omega$	2.12 ± 0.10	0.6/0.07	0.87 ± 0.25	0.01 ± 0.08	-2.3	
	$K^+ \phi$	0.12 ± 0.02	0.166/0.166	$0.182_{-0.27}^{+0.27} \pm 0.041$	0	-0.8	

Cheng, CWC 2019

all in units of 10^{-3}

	Mode	\mathcal{B}			a_{CP}^{dir}		HFLAV	
		ours	Qin+ 2014	exp	ours	Qin+ 2014		
$D^0 \rightarrow$	$\pi^+ \rho^-$	5.12 ± 0.29	4.74/4.66	5.15 ± 0.25	0.77 ± 0.22	-0.03		
	$\pi^- \rho^+$	10.21 ± 0.91	10.2/10.0	10.1 ± 0.4	-0.14 ± 0.04	-0.01		
	$\pi^0 \rho^0$	3.90 ± 0.26	3.55/3.83	3.86 ± 0.23	0.37 ± 0.15	-0.03		
	$K^+ K^{*-}$	1.68 ± 0.11	1.72/1.73	1.65 ± 0.11	-0.75 ± 0.37	-0.01		
	$K^- K^{*+}$	4.43 ± 0.31	4.37/4.37	4.56 ± 0.21	0.15 ± 0.04	0		
	$K^0 \bar{K}^{*0}$	0.27 ± 0.06	1.1/1.1	0.246 ± 0.048	-0.15 ± 0.21	-0.7		
	$\bar{K}^0 K^{*0}$	0.32 ± 0.09	1.1/1.1	0.336 ± 0.063	-0.34 ± 0.16	-0.7		
	$\pi^0 \omega$	0.12 ± 0.05	0.85/0.18	0.117 ± 0.035	-2.14 ± 0.95	0.02		
	$\pi^0 \phi$	1.22 ± 0.04	1.11/1.11	1.20 ± 0.04	0	-0.0002		
	$\eta \omega$	2.25 ± 0.14	2.4/2.0	1.98 ± 0.18	-0.38 ± 0.10	-0.1		
	$\eta' \omega$	0.01 ± 0.00	0.04/0.02	...	0.96 ± 0.66	2.2		
	$\eta \phi$	0.16 ± 0.02	0.19/0.18	0.167 ± 0.034	0	0.003	$-19 \pm 44 \pm 6$	
	$\eta \rho^0$	0.59 ± 0.07	0.54/0.45	...	0.10 ± 0.30	1.0		
	$\eta' \rho^0$	0.06 ± 0.01	0.21/0.27	...	0.16 ± 0.22	-0.1		
$D^+ \rightarrow$	$\pi^+ \rho^0$	0.61 ± 0.10	0.42/0.58	0.83 ± 0.15	2.20 ± 1.38	0.5		
	$\pi^0 \rho^+$	4.53 ± 0.64	2.7/2.5	...	0.49 ± 0.37	0.2		
	$\pi^+ \omega$	0.26 ± 0.07	0.95/0.80	0.28 ± 0.06	0.74 ± 2.03	-0.05		
	$\pi^+ \phi$	6.29 ± 0.20	5.65/5.65	5.68 ± 0.11	0	-0.0001		
	$\eta \rho^+$	1.02 ± 0.34	0.7/2.2	...	1.78 ± 0.69	-0.6		
	$\eta' \rho^+$	1.03 ± 0.11	0.7/0.8	...	0.08 ± 0.11	0.5		
	$K^+ \bar{K}^{*0}$	3.82 ± 0.25	3.61/3.60	$3.83^{+0.14}_{-0.21}$	-1.06 ± 0.30	0.2		
	$\bar{K} K^{*+}$	9.80 ± 0.41	11/11	34 ± 16	0.10 ± 0.04	0.04		
	$D_s^+ \rightarrow$	$\pi^+ K^{*0}$	3.65 ± 0.24	2.52/2.35	2.13 ± 0.36	1.05 ± 0.30	-0.1	
		$\pi^0 K^{*+}$	1.02 ± 0.07	0.8/1.0	...	1.15 ± 0.40	-0.2	
$K^+ \rho^0$		2.10 ± 0.10	1.9/2.5	2.5 ± 0.4	-0.08 ± 0.07	0.3		
$K^0 \rho^+$		11.47 ± 0.48	9.1/9.6	...	-0.08 ± 0.04	0.3		
ηK^{*+}		0.64 ± 0.20	0.2/0.2	...	0.10 ± 0.48	1.1		
$\eta' K^{*+}$		0.33 ± 0.02	0.2/0.2	...	-0.12 ± 0.13	-0.5		
$K^+ \omega$		2.12 ± 0.10	0.6/0.07	0.87 ± 0.25	0.01 ± 0.08	-2.3		
$K^+ \phi$		0.12 ± 0.02	0.166/0.166	$0.182^{27} \pm 0.041$	0	-0.8		

Cheng, CWC 2019

modes of interest,
with sufficiently large
BR's and CPA's.

all in units of 10^{-3}

	Mode	\mathcal{B}			$a_{\text{CP}}^{\text{dir}}$		HFLAV	
		ours	Qin+ 2014	exp	ours	Qin+ 2014		
$D^0 \rightarrow$	$\pi^+ \rho^-$	5.12 ± 0.29	4.74/4.66	5.15 ± 0.25	0.77 ± 0.22	-0.03		
	$\pi^- \rho^+$	10.21 ± 0.91	10.2/10.0	10.1 ± 0.4	-0.14 ± 0.04	-0.01		
	$\pi^0 \rho^0$	3.90 ± 0.26	3.55/3.83	3.86 ± 0.23	0.37 ± 0.15	-0.03		
	$K^+ K^{*-}$	1.68 ± 0.11	1.72/1.73	1.65 ± 0.11	-0.75 ± 0.37	-0.01		
	$K^- K^{*+}$	4.43 ± 0.31	4.37/4.37	4.56 ± 0.21	0.15 ± 0.04	0		
	$K^0 \bar{K}^{*0}$	0.27 ± 0.06	1.1/1.1	0.246 ± 0.048	-0.15 ± 0.21	-0.7		
	$\bar{K}^0 K^{*0}$	0.32 ± 0.09	1.1/1.1	0.336 ± 0.063	-0.34 ± 0.16	-0.7		
	$\pi^0 \omega$	0.12 ± 0.05	0.85/0.18	0.117 ± 0.035	-2.14 ± 0.95	0.02		
	$\pi^0 \phi$	1.22 ± 0.04	1.11/1.11	1.20 ± 0.04	0	-0.0002		
	$\eta \omega$	2.25 ± 0.14	2.4/2.0	1.98 ± 0.18	-0.38 ± 0.10	-0.1		
	$\eta' \omega$	0.01 ± 0.00	0.04/0.02	...	0.96 ± 0.66	2.2		
	$\eta \phi$	0.16 ± 0.02	0.19/0.18	0.167 ± 0.034	0	0.003	$-19 \pm 44 \pm 6$	
	$\eta \rho^0$	0.59 ± 0.07	0.54/0.45	...	0.10 ± 0.30	1.0		
	$\eta' \rho^0$	0.06 ± 0.01	0.21/0.27	...	0.16 ± 0.22	-0.1		
$D^+ \rightarrow$	$\pi^+ \rho^0$	0.61 ± 0.10	0.42/0.58	0.83 ± 0.15	2.20 ± 1.38	0.5		
	$\pi^0 \rho^+$	4.53 ± 0.64	2.7/2.5	...	0.49 ± 0.37	0.2		
	$\pi^+ \omega$	0.26 ± 0.07	0.95/0.80	0.28 ± 0.06	0.74 ± 2.03	-0.05		
	$\pi^+ \phi$	6.29 ± 0.20	5.65/5.65	5.68 ± 0.11	0	-0.0001		
	$\eta \rho^+$	1.02 ± 0.34	0.7/2.2	...	1.78 ± 0.69	-0.6		
	$\eta' \rho^+$	1.03 ± 0.11	0.7/0.8	...	0.08 ± 0.11	0.5		
	$K^+ \bar{K}^{*0}$	3.82 ± 0.25	3.61/3.60	$3.83^{+0.14}_{-0.21}$	-1.06 ± 0.30	0.2		
	$\bar{K} K^{*+}$	9.80 ± 0.41	11/11	34 ± 16	0.10 ± 0.04	0.04		
	$D_s^+ \rightarrow$	$\pi^+ K^{*0}$	3.65 ± 0.24	2.52/2.35	2.13 ± 0.36	1.05 ± 0.30	-0.1	
		$\pi^0 K^{*+}$	1.02 ± 0.07	0.8/1.0	...	1.15 ± 0.40	-0.2	
$K^+ \rho^0$		2.10 ± 0.10	1.9/2.5	2.5 ± 0.4	-0.08 ± 0.07	0.3		
$K^0 \rho^+$		11.47 ± 0.48	9.1/9.6	...	-0.08 ± 0.04	0.3		
ηK^{*+}		0.64 ± 0.20	0.2/0.2	...	0.10 ± 0.48	1.1		
$\eta' K^{*+}$		0.33 ± 0.02	0.2/0.2	...	-0.12 ± 0.13	-0.5		
$K^+ \omega$		2.12 ± 0.10	0.6/0.07	0.87 ± 0.25	0.01 ± 0.08	-2.3		
$K^+ \phi$		0.12 ± 0.02	0.166/0.166	0.182 ± 0.041	0	-0.8		

Cheng, CWC 2019

predict $\Delta a_{\text{CP}}^{\text{dir}}(K^+ K^{*-} - \pi^+ \rho^-)$
to be $(-1.52 \pm 0.43) \times 10^{-3}$

modes of interest,
with sufficiently large
BR's and CPA's.

all in units of 10^{-3}

Summary

- The theory community has been facing serious challenges in the charm sector, mainly due to the **lack of a good effective theory**.
- A reliable, first-principle calculation of **long-distance, nonperturbative dynamics** is missing, same for both perturbation- and symmetry-based approaches.
- Flavor SU(3) symmetry-breaking effects are introduced in a **data-driven** way.
- It is still an **open question** whether the observed CPA's can be accommodated within the SM or not.
- “New physics” in the CP violation of the D mesons here could mean either **new mechanisms within the SM** or **physics beyond the SM**.
- At the moment, **precision measurements** for the CPA's of more decay modes (also the BR's of some less well-determined modes) will check theory predictions and tell us **which theoretical approach is closer to the true story**.

Enjoy **FPCP**
(**Fun** **Puzzles** in **Charm** **Physics**)!